

# Structure elucidation and conformational properties of eprosartan a non peptide Angiotensin II AT<sub>1</sub> antagonist

Panagiotis Zoumpoulakis<sup>a</sup>, Simona Golic Grdadolnik<sup>b</sup>, John Matsoukas<sup>c</sup>,  
Thomas Mavromoustakos<sup>a,\*</sup>

<sup>a</sup> *Institute of Organic and Pharmaceutical Chemistry, National Hellenic Research Foundation. Vas. Constantinou 48, Athens 11635, Greece*

<sup>b</sup> *National Institute of Chemistry, Hajdrihova 19, PO Box 30, SI-1115 Ljubljana, Slovenia*

<sup>c</sup> *Department of Chemistry, University of Patras, 26500 Patras, Greece*

Received 3 August 2001; received in revised form 4 September 2001; accepted 8 September 2001

## Abstract

A novel approach to treat hypertension is to interfere with the Renin-Angiotensin system (RAS) by blocking the binding of vasoconstrictive hormone Angiotensin II to the AT<sub>1</sub> receptor site. This approach led to the beneficial drug losartan (COZAAR) and other similar in structure to the antihypertensive drugs (sartans). In an effort to compare the stereoelectronic features of pharmacophoric segments of the different sartans, a research activity was initiated in our laboratory related to the conformational properties of these drugs. In a previous study, the structural features which determine the pharmacophoric segments of losartan were examined. In this study, the conformational properties of eprosartan (TEVETEN), a drug with fewer side effects, were examined. In addition, the superimposition ability of losartan and eprosartan with the peptide antagonist sarmesin was studied. © 2002 Elsevier Science B.V. All rights reserved.

**Keywords:** Antihypertensives; Eprosartan; Losartan; AT<sub>1</sub> antagonists; NMR; Molecular modeling

## 1. Introduction

Angiotensin II is an octapeptide, well known to exert its physiological effects on a G-protein-coupled receptor cloned from rat, pig and human libraries and is called AT<sub>1</sub> [1].

In an effort to obtain information on the regio-chemical and stereochemical requirements for

productive binding at the active site of the AT<sub>1</sub> receptor, an effort was made to study the conformational analysis of synthetic peptides and non-peptide mimetic AT<sub>1</sub> antagonists.

The conformational properties of the high binding affinity molecule losartan, to the AT<sub>1</sub> receptor have been studied already. In particular, the structural features which determine the pharmacophoric segments of losartan are examined. These are: (a) conformation of biphenyltetrazole; (b) orientation of hydroxymethylimidazole rela-

\* Corresponding author. Fax: +30-1-727-3872.

E-mail address: [tmavro@eie.gr](mailto:tmavro@eie.gr) (T. Mavromoustakos).

tive to the biphenyl template; and (c) the *n*-butyl chain conformation. Losartan was superimposed with C-terminal region of AT<sub>1</sub> antagonist sarmesin since its design was based on its similarity with side groups that constitute the C-terminal part of Angiotensin II. Superimposition of losartan with AT<sub>1</sub> antagonist sarmesin showed that: (i) losartan's hydroxymethylimidazole matched with sarmesin's imidazole of His<sup>6</sup>; (ii) losartan's *n*-butyl chain was in a spatial proximity with *n*-butyl chain of sarmesin's Ile<sup>5</sup> carbon chain; (iii) losartan's tetrazole was in close vicinity in space with sarmesin's isosteric carboxylate of Phe<sup>8</sup>; and (iv) losartan's spacer phenyl ring matched with Sarmesin's pyrrolidine group of Pro<sup>7</sup>. Interestingly, losartan mimics the  $\gamma$ -turn formed around Pro<sup>7</sup> in sarmesin [2]. Recently, similar superimposition study was sought with the c-[Sar<sup>1</sup>-Lys<sup>3</sup>-Glu<sup>5</sup>-Ile<sup>8</sup>] ANG II. From the different possible overlays, the best superimposition between the two molecules was achieved when the following groups were matched: (i) losartan's hydroxymethylimidazole with c-[Sar<sup>1</sup>-Lys<sup>3</sup>-Glu<sup>5</sup>-Ile<sup>8</sup>] ANG II His<sup>6</sup>; (ii) losartan's spacer phenyl ring with c-[Sar<sup>1</sup>-Lys<sup>3</sup>-Glu<sup>5</sup>-Ile<sup>8</sup>] ANG II pyrrolidine group of Pro<sup>7</sup>; and (iii) losartan's hydroxymethyl group with phenolic hydroxyl group of Tyr<sup>4</sup>. Losartan as sarmesin mimics the  $\gamma$ -turn formed around Pro<sup>7</sup> in c-[Sar<sup>1</sup>-Lys<sup>3</sup>-Glu<sup>5</sup>-Ile<sup>8</sup>] ANG II [3].

Our studies have been extended to the detailed conformational analysis of eprosartan. It is an effective blood pressure lowering agent. Compared to other sartans, eprosartan appears to possess unique actions among the AT<sub>1</sub> blockers. It was shown on animal study that eprosartan was far more effective than other AT<sub>1</sub> blockers at inhibiting sympathetic nervous system activity. This biological property for eprosartan is important due to the fact that increased sympathetic nervous system activity causes systolic hypertension which is often found in the elderly [4]. Recent data suggest that eprosartan may be beneficial in progressive renal disease and that its mechanism of action includes inhibition of cytokine production in addition to antihypertensive activity [5]. In comparison to other sartans, eprosartan shows fewer side effects. Thus, it is not metabolized significantly, requires once daily dosing, and needs no necessary dosage adjustment for patients with renal or hepatic dysfunction.

The present study will aid in exploring the conformational similarities and differences between the AT<sub>1</sub> antagonists losartan and eprosartan (Fig. 1). Their superimposition similarities and differences with C-terminal parts of sarmesin is studied. The final aim of these studies is to explore their conformational dynamic properties in membrane bilayers and docking to AT<sub>1</sub> receptor. These under progress studies may shed light to the molecular basis of their action.

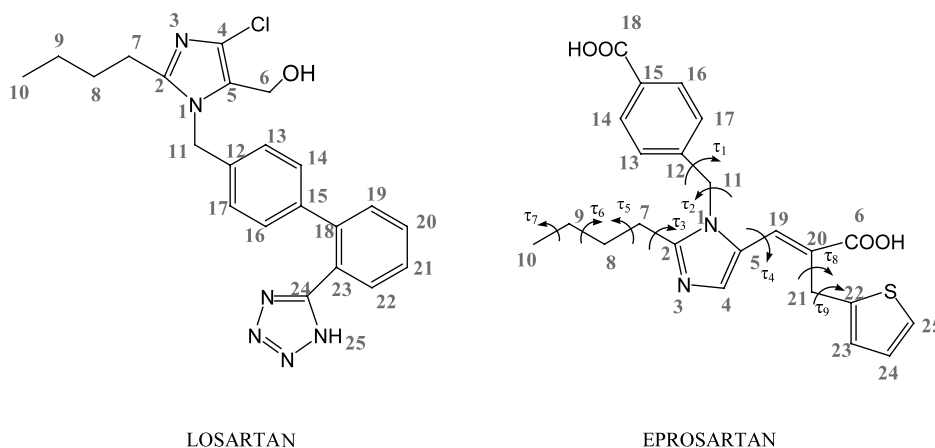


Fig. 1. Structure of the AT<sub>1</sub> antagonists losartan and eprosartan illustrating the atom nomenclature used in this study. The critical dihedral angles of eprosartan that determine its conformation are also labeled on the 2D structure of the molecule.

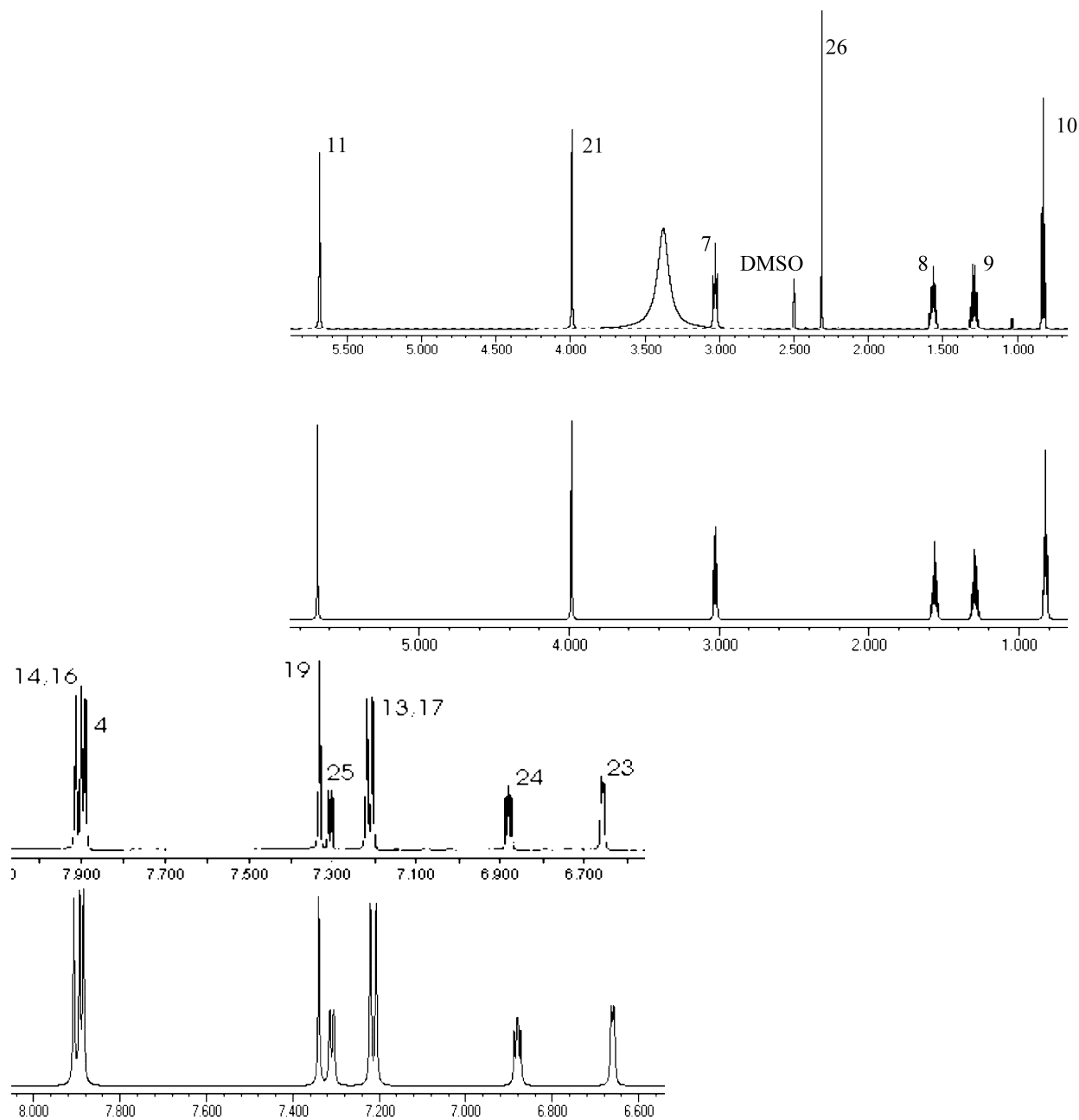


Fig. 2. <sup>1</sup>H-NMR spectra of eprosartan in DMSO recorded on a Varian INOVA 600 MHz spectrometer (top, experimental; bottom, simulated).

## 2. Materials and methods

### 2.1. Materials

DMSO- $d_6$  and ultra precision NMR tubes

Wilmad 535–5 mm (SPINTEC ROTOTEC) were used for the NMR experiments. Eprosartan was kindly offered by the company Solvay Pharmaceuticals.

Table 1

Assignment of the experimental  $^1\text{H}$  spectrum and calculated  $J$ -couplings based on its simulated  $^1\text{H}$  spectrum

Peak	Multiplicity (ppm) <sup>a</sup>	$J$ couplings	Peak	Multiplicity (ppm)	$J$ couplings
10	0.82 (t)	$J_{9-10} = 7$	11	5.68 (s)	
9	1.29 (h)	$J_{8-9} = 7$	23	6.66 (d)	$J_{23-24} = 3.71$
8	1.56 (p)	$J_{7-8} = 7$	24	6.88 (t)	$J_{24-25} = 5.48$
26	2.31 (s)		13, 17	7.21 (d)	$J_{13-14} = 8.00$ $J_{13-16} = 0.40$ $J_{13-17} = 0.71$
DMSO	2.49 (s)		25	7.31 (d)	$J_{23-25} = 1.36$
7	3.02 (t)		19	7.33 (s)	$J_{4-19} = 0.54$
H <sub>2</sub> O	3.37 (s)		4	7.89 (s)	
21	3.99 (s)	$J_{4-21} = 0.24$ $J_{21-23} = -0.96$	14, 16	7.91 (d)	$J_{14-17} = 0.40$ $J_{14-16} = 0.54$ $J_{16-17} = 8.00$

<sup>a</sup> s = singlet, d = doublet, t = triplet, p = pentaplet, h = hexaplet.

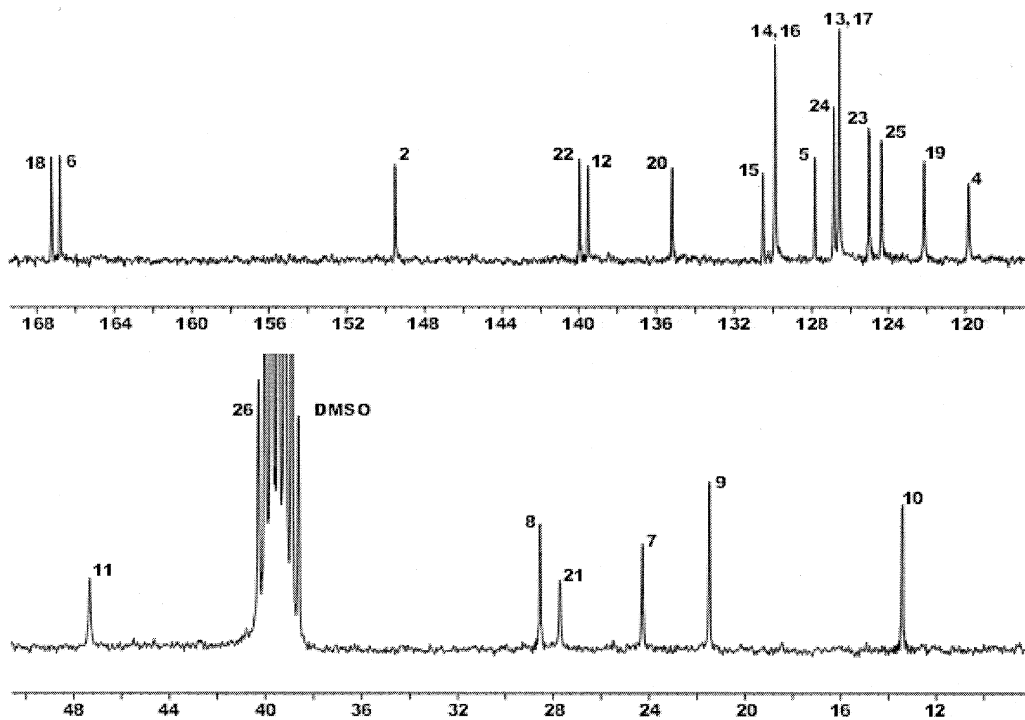


Fig. 3.  $^{13}\text{C}$ -NMR spectra of eprosartan in DMSO recorded on a Bruker AC 300MHz spectrometer.

Table 2  
Assignment of the  $^{13}\text{C}$  spectrum

Peak	ppm	Peak	ppm	Peak	ppm
10	13.1	19	122	20	135
9	21.2	25	124.4	12	139.5
7	24.1	23	125	22	140
21	27.5	13, 17	126.8	2	149.5
8	28.3	24	127	6	166.5
26	39.5	5	127.8	18	167
11	47	14, 16	130		
4	120	15	130.5		

Table 3  
Observed NOEs, their intensities and calculated distances in a low energy conformer

No.	Protons	Intensity <sup>a</sup>	Distance (Å)
1	8–11	L	3.990
2	7–11	S	2.856
3	7–(13, 17)	M	3.541
4	21–4	S	2.731
5	11–19	S	2.627

<sup>a</sup> L, light; M, medium; S, strong.

## 2.2. Nuclear magnetic resonance spectroscopy

The high resolution spectra were obtained using Varian INOVA 600MHz and Bruker AC 300 instruments at 298 K. All data were collected using pulse sequences and phase-cycling routines provided in the Bruker and Varian libraries of pulse programs. Data processing including sine-bell apodization, Fourier transformation, phasing, symmetrization and plotting were performed using Varian and Bruker software packages. The DQF-COSY,  $^1\text{H}$ – $^{13}\text{C}$  HSQC and  $^1\text{H}$ – $^{13}\text{C}$  HMBC experiments were performed with gradients [6–8]. The NOESY experiment was recorded using standard pulse sequence in the phase-sensitive mode and was measured at 150 ms mixing time. The  $^1\text{H}$  sweep width was 9820 at 600 MHz [9]. Typically, the homonuclear proton spectra were acquired with 4096 data points in  $t_2$ , 16–64 scans, 256–512 complex points in  $t_1$ , and a relaxation delay of 1–1.5 s. The  $^1\text{H}$ – $^{13}\text{C}$  HSQC spectra were recorded with 1024 data points in  $t_2$ , 16 scans per increment, 128 complex points in  $t_1$  and a relax-

ation delay of 1 s. The  $^{13}\text{C}$  spectral width was 20000 Hz. The  $^1\text{H}$ – $^{13}\text{C}$  HMBC spectra were recorded with 4096 data points in  $t_2$ , 64 scans per increment, 512 points in  $t_1$  and a relaxation delay of 1 s [10,11]. The  $^{13}\text{C}$  spectral width was 30000 Hz.

Data were processed and analyzed with FELIX software package from Biosym Technologies. Spectra were zero-filled two times and apodized with a squared sine bell function shifted by  $\pi/2$  in both dimensions. Distances were calculated from cross-peak volumes in NOESY spectra using the FELIX program. A pseudoatom for the methyl groups was added and the  $\pm 10\%$  was applied to the distance, to produce the upper and the lower limit constraints.

## 2.3. Simulations of NMR spectra

Computer calculations were performed using gNMR software v 4.1.0 by IvorySoft 1995–1999. Theoretical changes on proton chemical shifts and  $J$  couplings were made to resemble the experimental spectra. For better matching, simulations were made using full-lineshape iteration, iteration on linewidth and on the baseline.  $^1\text{H}$ -NMR spectrum from Varian 600 MHz spectrometer was used as a guide one. Linewidth was set to 2 during theoretical calculations.

## 2.4. Molecular dynamics

Computer calculations were performed on a Silicon Graphics using DISCOVER of INSIGHT II and conformational analysis of QUANTA softwares purchased from Molecular Simulation Incorporated (MSI). Eprosartan was first minimized and then subjected to molecular dynamics experiments to explore its lower energy conformers. Several simulations with different starting structures were carried out in DMSO. The molecule with all atoms treated explicitly was centered in a cubic box ( $x = y = z = 40$  Å) using three-dimensional periodic boundary conditions. Neighbor lists for calculation of non-bonded interactions were updated every 10 fs within a radius of 14 Å without use of switching functions. A time step of 1 fs was employed for the MD simulation. The

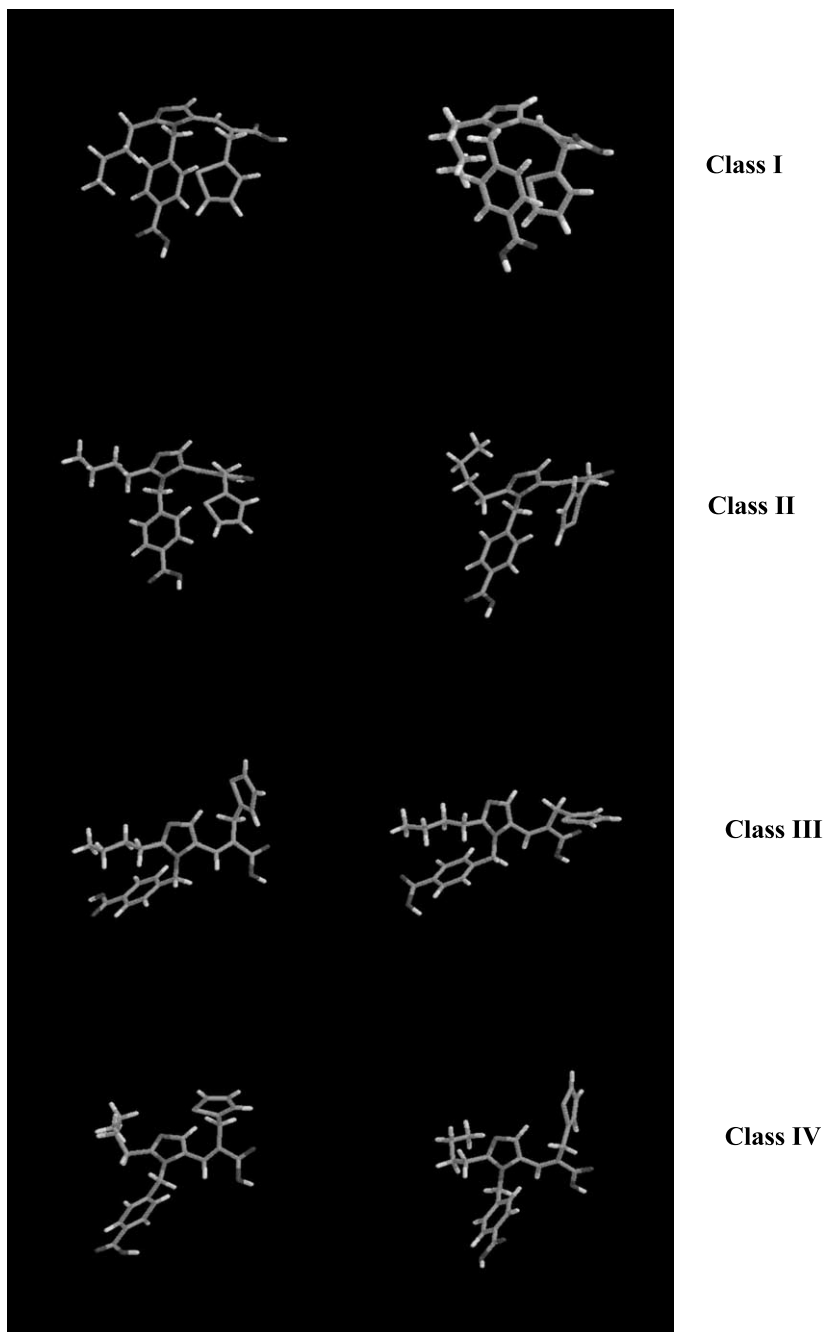


Fig. 4. Lowest energy conformers of eprosartan derived after using a combination of molecular dynamics under constraints and Monte Carlo conformational searches.

Table 4

Values of the dihedral angles of the lowest energy conformers generated by random sampling

Dihedrals	Class I		Class II		Class III		Class IV	
	Conf.1	Conf.2	Conf.3	Conf.4	Conf.5	Conf.6	Conf.7	Conf.8
$\tau_1$	119.0	-83.2	126.0	132.3	-120.4	49.3	-135.4	-38.0
$\tau_2$	-71.6	102.3	-80.4	-50.0	47.0	53.8	53.8	-75.8
$\tau_3$	94.6	-131.4	-88.3	-145.8	-103.2	-106.2	141.7	-79.4
$\tau_4$	-126.0	117.7	-130.4	-150.6	159.9	-139.8	-139.5	-150.3
$\tau_5$	-171.2	64.2	-179.9	77.3	170.9	169.5	-60.1	-63.4
$\tau_6$	175.5	-178.9	179.6	-69.4	-175.6	-174.5	-59.3	88.2
$\tau_7$	-179.0	179.9	-179.7	69.0	-59.7	-179.6	-175.6	175.5
$\tau_8$	98.5	-97.9	100.4	36.8	97.4	115.0	113.4	-99.5
$\tau_9$	-95.5	94.0	-95.6	41.3	-149.6	-90.8	-90.7	151.4

simulation protocol consisted of two minimization cycles (steepest descent and conjugate gradients), first with the solute fixed and then with all the atoms allowed to move freely. The convergence criterion was  $1 \text{ kcal } \text{Å}^{-1}$ . The initial MD phase of the calculation involved a gradual heating, starting from 100 K and then increasing to 150, 200, 250, and finally 300 K in steps of 0.5, 0.5, 5, 1, 5 ps, respectively, each by direct scaling of the velocities. The NMR derived distance restraints with a force constant of  $10 \text{ kcal mol}^{-1} \text{Å}^{-1}$  were applied during the complete simulation. Conformers derived during the 200 ps dynamics process were saved every 1 ps. The last 100 ps of the trajectory were used for analysis of NOE distance violations and dihedral angles. A Monte Carlo conformational search without constraints aided Molecular Dynamics experiment under constraints in an attempt to expand the conformational space and increase the probability to generate lower energy conformers which agree with the NOE data [6].

### 3. Results and discussion

#### 3.1. Structure identification of eprosartan

Fig. 2 depicts the  $^1\text{H-NMR}$  spectrum of eprosartan in DMSO solvent. Observed peaks are referenced to TMS. The assignment of the peaks is shown on the top of the spectrum. The proton chemical shifts of eprosartan are assigned follow-

ing standard procedures and using homonuclear DQF-COSY and NOESY in combination with  $^1\text{H-}^{13}\text{C}$  HSQC and  $^1\text{H-}^{13}\text{C}$  HMBC experiments (Table 1).

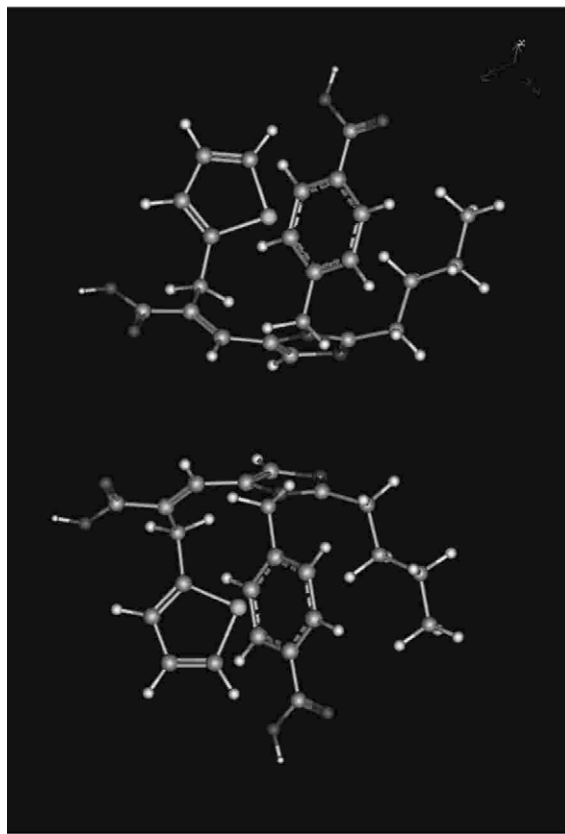


Fig. 5. Proposed bioactive enantiomers of eprosartan.

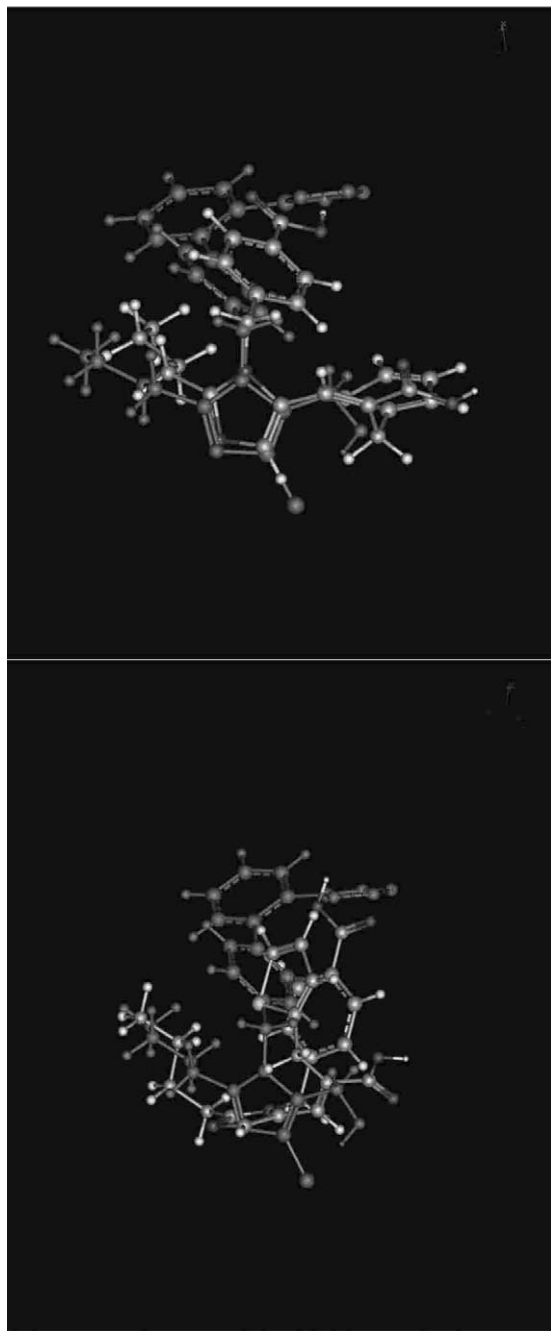


Fig. 6. Superimposition of the best-fit conformer of eprosartan with losartan.

The  $^{13}\text{C}$ -NMR signals of the  $\text{AT}_1$  antagonist were unambiguously assigned based on other similar molecules and the heteronuclear 2D spectra.

The  $^{13}\text{C}$ -NMR spectrum of eprosartan is shown in Fig. 3. The assignment of the peaks is shown above them (Table 2).

### 3.2. Conformational properties of eprosartan

In Table 3 are shown the NOEs which govern the conformational properties of eprosartan. The proton–proton distances, calculated from experimental NOESY spectra measured at 150 ms using the two-spin approximation and the integrated intensity of an aromatic pair of protons is assumed to have distance of 2.5 Å [7]. The observed NOEs 7–11, 7–13 (17) are critical for the conformational analysis of the studied molecule because they suggest a clustering between the butyl chain and the aromatic ring.

### 3.3. Conformational search

The 1000 resulted random conformers generated by Monte Carlo method were divided into four classes that agree with NOE data. The first class is characterized by a parallel relationship between butyl chain, the aromatic phenyl carboxylate and thiophene rings. In the second class only the two aromatic rings preserve this relationship while the butyl chain is extended perpendicular to these rings. In the third class phenyl carboxylate ring is parallel oriented with the butyl chain while thiophene is oriented perpendicular or parallel on the other side of the molecule. In the fourth class the two rings and butyl chain are far away. Pairs of the lowest energy conformers of these four classes are shown in Fig. 4 and their critical dihedral angles in Table 4. During the conformational search two conformers appeared with enantiomeric relationship even chiral center is missing from the structure (Fig. 5).

### 3.4. Superimposition between eprosartan and losartan (Fig. 6)

The eight low energy conformers of eprosartan derived from the combination of NMR spectroscopy and computational analysis were superimposed with losartan. The superimposition involved the following equivalent pharmacophore



segments: (i) eprosartans' nitrogen atoms of the imidazole ring with the corresponding ones of hydroxyimidazole ring of losartan; (ii) eprosartans' and losartans' terminal methyl groups; (iii) eprosartans' carboxylate group with the isosteric tetrazole of losartan; (iv) eprosartans' carboxyl group with losartans' hydroxymethyl group. The pair of class I showed the best overlapping. In the first overlay (top) with the conformer I, the four pharmacophore segments under comparison were matched nicely (RMSD = 1.31). In this comparison thiophene appeared with no other matched group. In

the second overlay (conformer II), the match of the four pharmacophores was inferior (RMSD = 1.97). However, the thiophene ring was in a close spatial proximity with the biphenyl system.

### 3.5. Superimposition of eprosartan with sarmesin (Fig. 7)

The two low energy conformers best approximated the four pharmacophore segments of losartan were superimposed with similar in feature aminoacid segments of sarmesin. This superimposi-

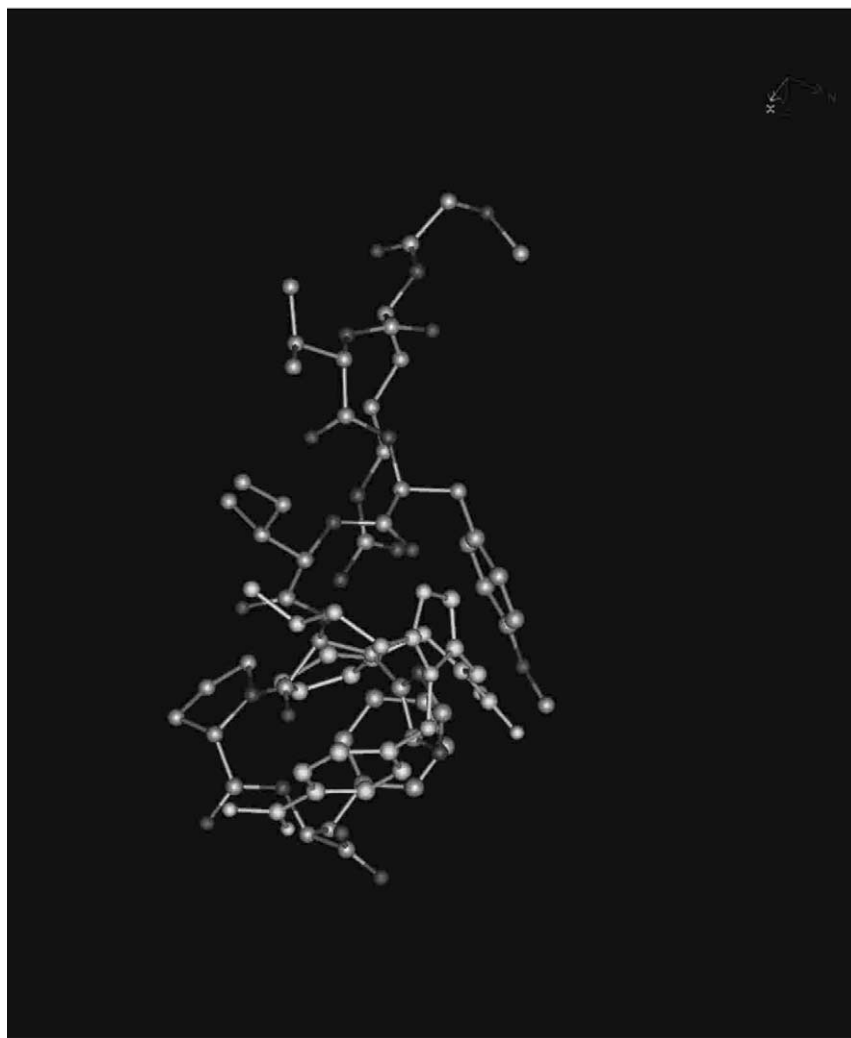


Fig. 7. Superimposition of the best-fit conformer of eprosartan with sarmesin.

tion is rationalized from the fact that AT<sub>1</sub> antagonists were designed and synthesized based on the C-terminal part of Angiotensin II. The best overlapping was achieved with conformer II of class I. In this superimposition the following equivalent groups were matched: (i) imidazole rings of His<sup>6</sup> and eprosartan; (ii) butyl chain of eprosartan with Ile<sup>5</sup> alkyl chain; (iii) acidic group attached to the phenyl ring of eprosartan with phenolic hydroxyl group of Tyr<sup>4</sup>. The RMSD found during the superimposition of the two molecules was 2.53 Å.

#### 4. Conclusions

Our laboratory is involved in the systematic exploration of the conformational properties of AT<sub>1</sub> antagonists in an attempt to comprehend their stereoelectronic properties that govern their antihypertensive properties.

This program aims: (i) to explore the lowest energy conformers of AT<sub>1</sub> antagonists using a combination of 2D NMR spectroscopy and computational analysis; these conformers may have higher probability to block AT<sub>1</sub> receptor's activation; (ii) to study the interactions of these drugs with membranes. Such research activities with losartan are already in progress; (iii) to dock the low energy conformers in AT<sub>1</sub> receptor. The anchoring of pharmacophore segments in the receptor may determine the molecular requirements for bioactivity and may lead to novel structures that possess better activity.

The research plan is rationalized from the fact that AT<sub>1</sub> antagonists act on the membrane helices of AT<sub>1</sub> receptors. Therefore, the mechanism of action of these molecules is energetically favored to involve their incorporation and then diffusion into membrane bilayers to reach the receptor site.

The obtained results show structural similarities between the pharmacophore segments of losartan and eprosartan. These can be summarized to: (i) the lowest energy conformers adopt close proximity of their isosteric acid moieties, of the aromatic phenyl carboxylate and biphenyl tetrazole, of the imidazole rings and their butyl chains; (ii) eprosartan appears more flexible and can adopt low energy conformers with thiophene to ap-

proach the biphenyl ring of losartan; (iii) both molecules appear to have low energy enantiomers with different superimposition capability onto sarmesin peptide. This may point out the importance of the chirality of these molecules in approaching the AT<sub>1</sub> receptor.

In addition, the superimposition of eprosartan with sarmesin, a peptide antagonist reveals several common features: (i) the two acidic moieties of eprosartan approach the C-terminal carboxylate group and phenolic hydroxyl group of Tyr<sup>4</sup>; (ii) the two phenyl rings of eprosartan are in a spatial proximity with phenyl rings of Phe<sup>8</sup> and Tyr<sup>4</sup>; (iii) imidazole rings of eprosartan and His<sup>6</sup> are also in close proximity; (iv) the butyl chain of eprosartan approaches Ile<sup>5</sup>.

The nice matching of these equivalent groups may explain the bioactivity of AT<sub>1</sub> antagonists. In addition, optimization of the RMSD values in the overlays of AT<sub>1</sub> antagonists with Sarmesin may lead to more bioactive drugs. A synthetic activity was initiated with the design of molecules which have better overlay with sarmesin compared to sartans.

#### Acknowledgements

This work was supported by the Ministry of Energy and Technology of Greece (EPET II/115, PENED 2001), Workpackage WP9 'Conformational analysis of peptidomimetic drugs' of the Program of the Center of Excellence at National Institute of Chemistry in Ljubljana Slovenia sponsored by European Commission, contract no: ICA1-CT-2000-70034.

#### References

- [1] M. De Gasparo, K.J. Catt, T. Inagami, J.W. Wright, Th. Unger, *Pharmacol. Rev.* 52 (2000) 415–472.
- [2] T. Mavromoustakos, A. Kolocouris, M. Zervou, P. Roumelioti, J. Matsoukas, R. Weisemann, *J. Med. Chem.* 42 (1999) 1714–1722.
- [3] L. Polevaya, T. Mavromoustakos, P. Zoumboulakis, S.G. Grdadolnik, P. Roumelioti, N. Giatas, Ilze Mutule, T. Keivish, D. Vlahakos, E. Iliodromitis, D. Kremastinos, *Bioorg. Med. Chem.* 9 (2001) 1639–1647.

- [4] J.C. Song, C.M. White. Pharmacologic, pharmacokinetic, and therapeutic differences among angiotensin II receptor antagonists. *Pharmacotherapy* 20 (2000) 130–139.
- [5] V.Y. Wong, N.J. Laping, L.C. Contino, B.A. Olson, E. Grygielko, D.P. Brooks, *Physiol. Genomics* 4 (2000) 35–42.
- [6] M. Rance, O.W. Sorensen, G. Bodenhausen, G. Wagner, R.R. Ernst, K. Wutrich, *Biochem. Biophys. Res. Commun.* 117 (1983) 479–485.
- [7] G. Bodenhausen, D.J. Ruben, *Chem. Phys. Lett.* 69 (1980) 185–189.
- [8] W. Willker, D. Leibfritz, R. Kerrsebaum, W. Bermel, *Magn. Reson. Chem.* 31 (1983) 479–485.
- [9] J. Jeener, B.H. Meier, P. Bachmann, R.R. Ernst, *J. Chem. Phys.* 71 (1979) 4546–4553.
- [10] A. Bax, M.F. Summers, *J. Am. Chem. Soc.* 108 (1986) 2093–2094.
- [11] W. Bermel, K. Wagner, C. Griesinger, *J. Magn. Reson.* 83 (1989) 223–232.